JOURNAL OF GUIDANCE, CONTROL, AND DYNAMICS
Vol. 15, No. 2, March-April 1992

Optimal Output Feedback for Linear Time-Periodic Systems

Anthony J. Calise,* Mark E. Wasikowski,† and Daniel P. Schrage‡
Georgia Institute of Technology, Atlanta, Georgia 30332

An approach is developed for applying optimal output feedback control theory to the design of fixed gain controllers for time-periodic systems. Constant feedback gains based on plant outputs are calculated by minimizing a linear quadratic performance cost functional. A solution algorithm is developed using Floquet-Lyapunov theory and a generalized harmonic expansion technique. The theory is applied to the control of a helicopter rotor blade in forward flight through individual blade control. It is shown that constant gain output feedback can be used to augment the stability of the resulting time-periodic system, with the potential for greatly reducing the implementation complexity.

Introduction

THE primary purpose of this paper is to present a general framework for applying output feedback techniques to linear time-periodic systems. The motivation for such an approach is, in part, to reduce the control implementation requirements. The use of constant gain optimal output feedback in designing active feedback controllers provides many advantages over existing linear quadratic Gaussian (LQG) design methods. In particular, an on-line observer is not required, and the method can be extended to include compensator design wherein the order of the compensator may be prespecified during the design process. Unneeded feedback channels may also be eliminated.[1] The number of sensors may be reduced while eliminating the need to estimate all of the unmeasurable states in real time. Recently, efficient compensator design formulations have been developed for linear time-invariant systems including robustness considerations for both unstructured uncertainty and parametric uncertainty.[2,3]

The potential advantages of designing a fixed-order linear time-invariant controller are especially appealing for systems whose equations of motion are characterized by linear periodic coefficient dynamics. Aerospace applications include helicopter forward flight stability and control and satellite orbital stability problems. For helicopter aeromechanical and aeroelastic stability and control applications, the number of states required to model the system accurately continues to increase as research in structural elasticity, dynamic inflow, and aeroelasticity progresses. However, the feasibility and cost effectiveness of measuring/estimating all of the higher frequency structural elastic and dynamic inflow positions and rates for helicopter rotors in real time in an operational environment is questionable. This also drives the need for potential alternatives to the full state feedback solution. An output feedback approach provides additional flexibility in that higher fidelity state space physical models may be used for the control design.

The control design for both full state and output feedback methods are complicated by the period coefficients that describe the dynamics of the system. In helicopter applications, a multiblade coordinate (MBC) transformation has been employed.[4] If the periodic terms are neglected, then a constant coefficient system results as an approximation for analysis and design purposes and represents a reasonable approximation to the actual periodic system. However, from a theoretical standpoint, the MBC transformation is valid only for periodic systems with polar symmetry, which precludes its use in the analysis of practical applications such as automated track and balance, blade damage tolerance, and one damper inoperative in-plane stability. Also, the MBC approximation is subject to increasing inaccuracy as the magnitude of the periodic terms increases. Thus, the MBC approximation may not be adequate for rotor blade control laws designed for high-speed rotorcraft vibration and loads reduction and high-speed aeroelastic stability.

Previous efforts in applying modern feedback control to time-periodic systems[5-8] have investigated pole placement and model following. In general, both methods involve measuring and/or estimating all of the periodic states of the plant. This is a direct consequence of employing a control structure in which a linear combination of all of the rotor states is used to generate the feedback signal. LQG design methods for a time-periodic plant implies solving a periodic Ricatti equation and implementing periodic feedback gains. In general, this implies that an observer with periodic filter gains must also be implemented in real time to estimate all of the unmeasurable states.

Depending on the level of periodicity in the plant, the states may have significant higher harmonic content. This is produced by the contributions from the infinite number of higher frequency poles, which is characteristic of periodic systems. The standard LQG approach penalizes the states equally over all frequencies. This may result in unacceptably high feedback gains and bandwidth for the closed-loop system. The present formulation penalizes the response and control envelopes rather than the actual time histories. The envelope is obtained using Floquet-Lyapunov theory. This envelope also corresponds to a natural mode of the system, thereby enabling one to distribute the performance penalty over certain frequencies of interest and to choose the state and control weighting matrices accordingly.

The present effort examines the class of output feedback gains that are time invariant. The motivation for this initial investigation is that it can later be extended to include fixed order time-invariant dynamic compensation, along similar lines that have been pursued for time-invariant systems.[2,3] First, the problem statement is discussed. This is followed by a review of the applicable Floquet-Lyapunov theory. This theory provides the foundation for an optimal output feedback formulation. A sequential solution algorithm and computationally efficient numerical procedures are then presented. Next, the computational stability and efficiency of the solution algorithm and numerical procedures are demonstrated, and a specific design for improving the in-plane stability of a helicopter rotor blade in forward flight is treated.

Presented as Paper 89-3574 at the AIAA Guidance, Navigation, and Control Conference, Boston, MA, Aug. 14-16, 1989; received Jan. 16, 1990; revision received March 12, 1991; accepted for publication April 5, 1991.

*Professor, School of Aerospace Engineering. Associate Fellow AIAA.

†Graduate Fellow; currently, Research Engineer, Georgia Tech Research Institute. Member AIAA.

‡Professor. Member AIAA.

Problem Statement

Consider a linearized time-periodic system of the form

$$\dot{x}(\Psi) = A(\Psi)x(\Psi) + B(\Psi)u(\Psi), \qquad x(0) = x_0 \tag{1}$$

where $x \in \mathfrak{R}^n$ and $u \in \mathfrak{R}^m$, where

$$A(\Psi) = A(\Psi + \Omega T)$$

$$B(\Psi) = B(\Psi + \Omega T) \tag{2}$$

and $\dot{x}$ denotes $dx/d\Psi$. As expressed in Eq. (1), time is nondimensionalized by the fundamental frequency Ω. The output sensor measurements take the form

$$y(\Psi) = Cx(\Psi) \tag{3}$$

where $y \in \mathfrak{R}^p$. The constant gain feedback control based on the measurements is then

$$u(\Psi) = -Gy(\Psi) \tag{4}$$

Floquet-Lyapunov Theory

Floquet-Lyapunov theory has been used in many investigations of rotor blade stability and control design.[5-14] Since Eq. (1) is linear, the homogeneous solution can be written in the form

$$x(\Psi) = \Phi(\Psi,0)x(0) \tag{5}$$

where the columns of the state transition matrix remain linearly independent over the domain of the solution. The state transition matrix satisfies

$$\dot{\Phi}(\Psi,0) = A(\Psi)\Phi(\Psi,0), \qquad \Phi(0,0) = I \tag{6}$$

The solution to Eq. (6) can be constructed from the multivariable Floquet-Lyapunov Theorem,[15]

$$\Phi(\Psi,0) = M(\Psi)e^{\Lambda\Psi}M^{-1}(0) \tag{7}$$

Thus, the solution can be separated into an exponential form and a purely periodic modulator. The Floquet decomposition is the analog of a modal decomposition for the time-invariant case. $M(\Psi)$ represents the matrix of periodic complex eigenvectors with period T, and Λ is a constant diagonal complex matrix of Poincare (characteristic) exponents. Thus, the stability of Eq. (1) can be determined from Λ. Since M is periodic,

$$\Phi(\Omega T, 0) = M(0)e^{\Lambda\Omega T}M^{-1}(0) \tag{8}$$

The Poincare exponents can be calculated from the eigenvalues λ_j of $\Phi(\Omega T, 0)$ as,

$$\Lambda_j = \frac{1}{2\Omega T}\ell n\{\mathfrak{I}^2(\lambda_j) + \mathfrak{R}^2(\lambda_j)\} + i\frac{\tan^{-1}\{[\mathfrak{I}(\lambda_j)]/[\mathfrak{R}^2(\lambda_j)]\}}{\Omega T} + in_j \tag{9}$$

The imaginary part is nonunique, as n_j may be any integer. This results in an infinite multiplicity of roots, which is characteristic of periodic systems. However, n_j may be chosen to minimize the level of periodicity in $M(\Psi)$. This particular choice of n_j corresponds to the mode that dominates the system response. The effect of the choice of n_j will be addressed later in the application section.

Knowledge of the state transition matrix over one period determines the stability of the periodic system. Therefore, using the similarity transformation

$$x(\Psi) = M(\Psi)\eta(\Psi) \tag{10}$$

on Eq. (1) results in

$$\dot{\eta}(\Psi) = M^{-1}(\Psi)[A(\Psi)M(\Psi) - \dot{M}(\Psi)]\eta(\Psi) + M^{-1}(\Psi)B(\Psi)u(\Psi) \tag{11}$$

However, from Eqs. (6) and (7),

$$\dot{M}(\Psi) = A(\Psi)M(\Psi) - M(\Psi)\Lambda \tag{12}$$

Note that the inverse of the modal matrix satisfies

$$\dot{M}^{-1}(\Psi) = -M^{-1}(\Psi)A(\Psi) + \Lambda M^{-1}(\Psi) \tag{13}$$

Substituting Eq. (12) into Eq. (11) and Eq. (10) into Eq. (3) yields

$$\dot{\eta}(\Psi) = \Lambda\eta(\Psi) + M^{-1}(\Psi)B(\Psi)u(\Psi) \tag{14}$$

$$y(\Psi) = CM(\Psi)\eta(\Psi) \tag{15}$$

Thus, the transformation provides not only modal decoupling, but reduces the homogeneous portion of the open-loop response envelope to constant coefficient dynamic equations. Note that $\eta(\Psi)$ can be viewed as the modulator or envelope of the response for $x(\Psi)$ in Eq. (10). However, the closed-loop system defined by Eqs. (4), (14), and (15) is also a periodic system due to the feedback control term. This greatly complicates the closed-loop system design.

Controller Design Formulation

A technique is introduced to calculate the optimal output feedback gain matrix that minimizes a performance cost functional penalizing the transformed Floquet states (envelope of the closed-loop system response) and the control. First consider

$$J = E_{\eta o}\left\{\int_0^\infty (\eta^T Q\eta + u^T Ru)\, d\Psi\right\} \tag{16}$$

where the expectation is taken over an assumed distribution of initial conditions. The difficulty that immediately arises is

$$u^T Ru = \eta^T M^T(\Psi)C^T G^T RGCM(\Psi)\eta$$

$$= \eta^T Q_1(\Psi)\eta \tag{17}$$

which introduces periodic coefficient terms. Thus, we consider a modified performance index that penalizes the envelope of the control response. The envelope term is defined by using the constant part of $Q_1(\Psi)$

$$\{u^T Ru\}_e = \eta^T\left[\sum_{i=1}^{2h+1} k_i E_{Ci}^T G^T RGE_{Ci}\right]\eta \tag{18}$$

where

$$k_i = \begin{cases} 1 & \text{if } i = 1 \\ \frac{1}{2} & \text{otherwise} \end{cases} \tag{19}$$

and h is the number of harmonics used. The summation in Eq. (18) accounts for higher harmonic contributions to the constant part acting through the constant feedback gain matrix G. The matrices E_{Ci} are formed from the ith $(n \times p)$ partitioned block of E_C, defined as

$$E_C = C\tilde{M} \tag{20}$$

where $\tilde{M}$ is an $n \times (2h+1)n$ matrix formed from the cosine and sine harmonic components of $M(\Psi)$

$$\tilde{M} = \left[M_{0c} \vdots M_{1c} \vdots \cdots \vdots M_{hc} \vdots M_{1s} \vdots \cdots \vdots M_{hs}\right] \tag{21}$$

To obtain the terms in Eq. (21), $M(\Psi)$ is expanded in a Fourier series as

$$M(\Psi) = \sum_{i=0}^{h} [M_{ic} \cos(i\Psi) + M_{is} \sin(i\Psi)] \tag{22}$$

Using Eq. (18) in Eq. (16), the modified performance index may be expressed as

$$J_e = E_{\eta o}\left\{\int_0^{\infty} \eta^T \left(Q + \sum_{i=1}^{2h+1} k_i E_{Ci}^T G^T R G E_{ci}\right)\eta \, d\Psi\right\} \tag{23}$$

The performance index in Eq. (23) is minimized subject to the following periodic closed-loop system dynamic matrix

$$\dot{\eta} = A_c(\Psi)\eta \tag{24}$$

where

$$A_c = \Lambda - M^{-1}(\Psi)B(\Psi)GCM(\Psi) \tag{25}$$

At this stage, it can be seen that the closed-loop system in the transformed Floquet states is again a periodic system due to the effect of the feedback gain matrix. In order to apply the theory of constant gain output feedback, it is necessary to consider only the constant part of A_c

$$\bar{A}_c = \Lambda - \sum_{i=1}^{2h+1} k_i E_{Bi} G E_{Ci} \tag{26}$$

It should be noted that a G minimizing Eq. (23) subject to the modified constraint

$$\dot{\eta} = \bar{A}_c \eta \tag{27}$$

does not guarantee stability of Eq. (24). However, the effect of this approximation will later be removed in the iteration process presented in the next section. The matrices E_{Bi} are formed from the ith $(n \times m)$ partitioned block of E_B, defined as

$$E_B = \tilde{M}^{-1}\Pi(B) \tag{28}$$

where $\tilde{M}^{-1}$ is an $n \times (2h+1)n$ matrix formed similar to $\tilde{M}$ in Eq. (21), and the $(2h+1)n \times (2h+1)m$ Fourier product operator matrix $\Pi(B)$ is formed similar to that of Ref. 16:

$$\Pi(B) = \frac{1}{2}\begin{bmatrix} \Pi(B)^{++} & \Pi(B)^{+-} \\ \Pi(B)^{-+} & \Pi(B)^{--} \end{bmatrix} \tag{29}$$

with

$$\Pi(B)^{++} = \{B_{cl} + B_{cl}^T + B_{cu} + [B_{0c}]\} \tag{30}$$

$$\Pi(B)^{+-} = \{-B_{sl} + B_{sl}^T + B_{su}\} \tag{31}$$

$$\Pi(B)^{-+} = \{B_{sl} - B_{sl}^T + B_{su}\} \tag{32}$$

$$\Pi(B)^{--} = \{B_{cl} + B_{cl}^T - B_{cu} + [B_{0c}]\} \tag{33}$$

where the submatrices are defined as

$$B_{cl} = \begin{bmatrix} B_{0c} & 0 & 0 & \cdots & 0 & 0 \\ B_{1c} & B_{0c} & 0 & \cdots & 0 & 0 \\ B_{2c} & B_{1c} & B_{0c} & \cdots & 0 & 0 \\ \vdots & \vdots & \vdots & \ddots & \vdots & \vdots \\ B_{hc} & B_{(h-1)c} & B_{(h-2)c} & \cdots & B_{1c} & B_{0c} \end{bmatrix} \tag{34}$$

$$B_{cu} = \begin{bmatrix} B_{0c} & B_{1c} & B_{2c} & \cdots & B_{(h-1)c} & B_{hc} \\ B_{1c} & B_{2c} & & \cdots & B_{hc} & 0 \\ B_{2c} & & & & & 0 \\ \vdots & \vdots & & & & \vdots \\ B_{(h-1)c} & B_{hc} & & & & \vdots \\ B_{hc} & 0 & 0 & \cdots & \cdots & 0 \end{bmatrix} \tag{35}$$

$$[B_{0c}] = \begin{bmatrix} B_{0c} & 0 & \cdots & 0 \\ 0 & 0 & \cdots & 0 \\ \vdots & \vdots & \ddots & \vdots \\ 0 & 0 & \cdots & 0 \end{bmatrix} \tag{36}$$

The sine component matrices are defined in the same manner by substituting the sine component harmonic amplitude matrices for their cosine counterparts. The expression for E_B in Eq. (28) is much more complicated than that for E_C in Eq. (20) because both M^{-1} and B are periodic, whereas C is constant. The summations in Eqs. (30-33) efficiently account for the generation of subharmonic and superharmonic terms when M^{-1} and B are multiplied together.

The minimization of Eq. (23) subject to Eq. (27) can be cast as a static optimization problem similar to that of Ref. 1. The first-order necessary conditions for optimality result from minimizing the Lagrangian

$$\mathfrak{L}(G,K,L) = \text{tr}[K + \mathfrak{F}(G,K)L^T] \tag{37}$$

with respect to G, K, and L, where K is the unique solution of

$$\mathfrak{F}(G,K) = \bar{A}_c^T K + K\bar{A}_c + Q + \sum_{i=1}^{2h+1} k_i E_{Ci}^T G^T R G E_{Ci} \tag{38}$$

and L is the matrix of Lagrange multipliers. The initial conditions are assumed uniformly distributed over the unit sphere. The resulting necessary conditions are

$$\bar{A}_c^T K + K\bar{A}_c + Q + \sum_{i=1}^{2h+1} k_i E_{Ci}^T G^T R G E_{Ci} = 0 \tag{39}$$

$$L\bar{A}_c^T + \bar{A}_c L + I = 0 \tag{40}$$

$$G = R^{-1}\left[\sum_{i=1}^{2h+1} k_i E_{Bi}^T K L E_{Ci}^T\right]\left[\sum_{j=1}^{2h+1} k_j E_{Cj} L E_{Cj}^T\right]^{-1} \tag{41}$$

Numerical Procedures

In this section, a generalized harmonic expansion technique is introduced to calculate the Floquet transformation harmonics, as required by Eqs. (20) and (28). An equivalent real form of the Floquet transformation is also used to avoid numerical computations with complex quantities. An iterative numerical algorithm is presented to calculate the feedback gain matrix. Finally, the iterative procedure is modified to remove the approximation in Eq. (26).

The Floquet transformation harmonics $\tilde{M}$ and $\tilde{M}^{-1}$ are required to calculate the feedback gain matrix. One straightforward approach[5] to calculate $\tilde{M}$ would be to integrate Eq. (12) through one period and perform n^2 fast Fourier transforms (FFT) on the resulting time series. The inverse transformation $M(\Psi)^{-1}$ would be calculated in a similar manner by integrating the adjoint system or by taking a numerical inverse at each time step. The harmonic content of the inverse transformation $\tilde{M}^{-1}$ would be calculated by performing another n^2 FFT. Note, however, that only the harmonics of the transformation are required for the control design. Calculating a time history is an intermediate step and is not required.

A generalized harmonic expansion method is introduced here to solve for the harmonics of the transformation directly. The modal matrix initial and final conditions over the fundamental period are matched, as well as a finite number of their derivatives. This permits direct closed-form algebraic computation of approximate solutions to the harmonics of the transformations.

The elements of M are expressed in a Fourier series as defined in Eq. (22). Arranging the harmonic coefficients as defined in Eq. (21) while matching initial conditions and their $2h$ derivatives defined by Eq. (12) yields the following system of linear equations:

$$\tilde{M}I_B = \left[M_o \vdots M_o^{(1)} \vdots \cdots \vdots M_o^{(2h)}\right] \tag{42}$$

where $M_o^{(i)}$ denotes the ith derivative of $M(\Psi)$ evaluated at $\Psi = 0$. In Eq. (42), I_B is a structurally nonsingular matrix obtained from evaluating the derivatives of the orthogonal harmonic shape functions in Eq. (21) at the start of the fundamental period

$$I_B = \begin{bmatrix} I & 0 & 0 & 0 & 0 & & 0 \\ \vdots & \vdots & -I & \vdots & I & & I \\ \vdots & \vdots & -2^2 I & \vdots & 2^4 I & & 2^{2h} I \\ \vdots & \vdots & \vdots & \vdots & \vdots & & \vdots \\ I & 0 & -h^2 I & 0 & h^4 I & \cdots & h^{2h} I \\ 0 & I & 0 & -I & 0 & & 0 \\ \vdots & 2I & \vdots & -2^3 I & \vdots & & 0 \\ \vdots & \vdots & \vdots & \vdots & \vdots & & 0 \\ 0 & hI & 0 & -h^3 I & 0 & & 0 \end{bmatrix} \tag{43}$$

and the right-hand-side derivatives in Eq. (42) are obtained from the recursive formula

$$M_o^{(i)} = A_o M_o^{(i-1)} - M_o^{(i-1)}\Lambda + \sum_{j=1}^{i-1} c_{if} A_o^{(j)} M_o^{(i-1-j)}$$
$$i = 2, \ldots, 2h \tag{44}$$

which follows from repeated differentiations of Eq. (12) evaluated at $\Psi = 0$.

In solving for $\tilde{M}^{-1}$, Eqs. (42) and (43) are used with $\tilde{M}$ and $M_o^{(i)}$ replaced by $\tilde{M}^{-1}$ and $[M_o^{-1}]^{(i)}$, and Eq. (44) is replaced by its adjoint

$$[M_o^{-1}]^{(i)} = -[M_o^{-1}]^{(i-1)} A_o + \Lambda [M_o^{-1}]^{(i-1)}$$
$$- \sum_{j=1}^{i-1} c_{ij}{}^{i-1} [M_o^{-1}]^{i-1-j} A_o^{(j)}, \qquad i = 2, \ldots, 2h \tag{45}$$

The coefficients c_{ij} are obtained from the $j+1$ element of the ith row of Pascal's triangle, so that

$$c_{ij} = \begin{cases} c_{i-1,j-1} + c_{i-1,j} & \text{if } 1 < j < i-1 \\ c_{i-1,1} + 1 & \text{if } j = 1 \\ 1 & \text{if } j = i-1 \end{cases} \tag{46}$$

No numerical differentiation is required since Eq. (44) is recursive and the initial conditions for the modal matrix (M_o^o and $[M_o^o]^{-1}$) are obtained from the Floquet analysis. From Eq. (42), the harmonic coefficient matrices are found directly.

Numerical efficiency can be gained by using an equivalent real representation for Λ and $M(\Psi)$. In general, the Poincare exponents Λ (most conveniently put in diagonal form) and the periodic eigenvectors $M(\Psi)$ are complex. In an equivalent real form,[5] Λ is put into Jordan form with the complex eigenvalues arranged as follows:

$$\begin{bmatrix} \Re(\lambda_i) & \Im(\lambda_i) \\ -\Im(\lambda_i) & \Re(\lambda_i) \end{bmatrix} \tag{47}$$

with an associated reorganization of M. The same vector space is spanned using a real representation of the eigenvectors. All other equations remain unaltered. Using $\tilde{M}$ and M^{-1}, E_C and E_B are then calculated from Eqs. (20) and (28), respectively.

The necessary conditions are then solved to obtain the feedback gain matrix using a sequential algorithm of the form

(0) choose G_o such that $\bar{A}_c$ is stable; set $i = 0$
(1) solve Eqs. (39) and (40) for K_i and L_i
(2) evaluate

$$\Delta G = R^{-1}[\textstyle\sum_{j=1}^{2h+1} k_j E_{Bj}^T K_i L_i E_{cj}^T][\sum_{l=1}^{2h+1} k_l E_{Cl} L_i E_{cl}^T]^{-1} - G_i$$

(3) set $G_{i+1} = G_i + \alpha \Delta G_i$ for $0 < \alpha \leq 1$ such that $J_{i+1} < J_i$
(4) set $i = i + 1$ and go to step 1

Note that at each iteration the choice of α must be made such that G_{i+1} stabilizes $\bar{A}_c$ and is improving. If $\bar{A}_c$ can be stabilized by output feedback, then this process will converge.[1] A survey of methods for determining an initial stabilizing gain G_o is given in Ref. 17. We have adopted a simple approach that involves first shifting the eigenvalue of $\bar{A}_c$ so that they are all stable. The initial gain is set to zero, and during the iteration process, the shift is gradually removed until an initial stabilizing gain is found. A second problem that may arise in constant gain output feedback is the possible existence of more than one locally minimizing solution. The only recourse in this case is to investigate these solutions by starting the algorithm with different initial gains. However, this problem was not encountered in the numerical studies performed to date on periodic systems.

To eliminate the approximation in Eq. (26), an outer loop is added to the procedure. A perturbation to the feedback control is formed as

$$u = \bar{u} + \delta u \tag{48}$$

where

$$\bar{u} = -\bar{G}y \tag{49}$$

with $\bar{G}$ defined as the converged solution from the iteration process just defined. The perturbation in the control is defined as

$$\delta u = -\delta G y \tag{50}$$

A Floquet analysis and an associated generalized harmonic expansion is repeated on the closed-loop system

$$\dot{x} = [A(\Psi) - B(\Psi)\bar{G}C]x + B(\Psi)\delta u \tag{51}$$

to obtain a new estimate of the Poincare exponents Λ and modal matrices $\tilde{M}$ and $\tilde{M}^{-1}$. Substituting the control equation (48) into the original performance index (23) yields

$$J_e = E_{\eta o}\left\{\int_0^\infty \eta^T \bar{Q} \eta \, d\varphi\right\} \tag{52}$$

where

$$\bar{Q} = Q + \sum_{i=1}^{2h+1} k_i E_{Ci}^T \bar{G}^T R \bar{G} E_{Ci}$$
$$+ \sum_{j=1}^{2h+1} k_j E_{Cj}^T \delta G^T R \bar{G} E_{Cj}$$
$$+ \sum_{l=1}^{2h+1} k_l E_{Cl}^T \bar{G}^T R \delta G E_{Cl}$$
$$+ \sum_{s=1}^{2h+1} k_s E_{Cs}^T \delta G^T R \delta G E_{Cs} \tag{53}$$

with the dynamics given by

$$\dot{\eta} = \bar{A}_c \eta \tag{54}$$

where

$$\bar{A}_c = \Lambda - \sum_{i=1}^{2h+1} k_i E_{Bi} \delta G E_{Ci} \tag{55}$$

The resulting necessary conditions are slightly different from those obtained in Eqs. (39-41) due to the cross product terms that arise in Eq. (53)

$$\bar{A}_c^T K + K \bar{A}_c + Q + \sum_{i=1}^{2h+1} k_i E_{Ci}^T \bar{G}^T R \bar{G} E_{Ci}$$
$$+ \sum_{j=1}^{2h+1} k_j E_{Cj}^T \delta G^T R \bar{G} E_{Cj} + \sum_{i=1}^{2h+1} k_l E_{Cl}^T \bar{G}^T R \delta G E_{Cl}$$
$$+ \sum_{s=1}^{2h+1} k_s E_{Cs}^T \delta G^T R \delta G E_{Cs} = 0 \tag{56}$$

$$L\bar{A}_c^T + \bar{A}_c L + I = 0 \tag{57}$$

$$\delta G = R^{-1}\left[\sum_{i=1}^{2h+1} k_i E_{Bi}^T K L E_{Ci}^T\right]\left[\sum_{j=1}^{2h+1} k_j E_{Cj} L E_{Cj}^T\right]^{-1} - \bar{G} \tag{58}$$

The inner-loop iteration is repeated with Eq. (39) and Eq. (40) replaced by Eqs. (56) and (57) and with G_i now defined as δG_i and $\delta G_o = 0$. For the next outer loop, the control takes the form

$$u = -(\bar{G} + \delta G)y + \delta u \tag{59}$$

The outer loop is repeated until the solution converges (δG approaches zero).

Equation (59) is used to remove the approximation introduced by the use of $\bar{A}_c$ in Eq. (26), which approximates the closed-loop dynamics given by Eq. (25) as a time-invariant matrix. The outer-loop calculation transfers the effect of the periodic matrices $B(\Psi)$ and $M(\Psi)$, which act through the feedback gain matrix G, from the second term in Eq. (25) to the first term, Λ. This is accomplished by performing successive Floquet transformations on the closed-loop system defined by using the gain matrix from the preceding inner-loop calculation.

Thus, in each outer-loop calculation, A_c in Eq. (25) and $\bar{A}_c$ in Eq. (26) become

$$A_c = \Lambda - M^{-1}(\Psi)B(\Psi)\delta G C M(\Psi) \tag{60}$$

$$\bar{A}_c = \Lambda - \sum_{i=1}^{2h+1} k_i E_{Bi}\delta G E_{Ci} \tag{61}$$

As the outer-loop calculation converges, $\delta G \to 0$ and $\bar{A}_c$ approaches A_c. Convergence of the outer-loop calculation will be evaluated in the next section.

Examples

In forward flight, the dynamics of a helicopter rotor blade become time periodic due to the unsteady asymmetrical flow over the airfoil as it traverses the azimuth. For this example, the physical assumptions and derivation of the equations of motion are given in Refs. 13 and 14. Both rigid in-plane (lead-lag) and rigid out-of-plane (flap) dynamics are included in the model. The helicopter is first trimmed in forward flight using a moment trim procedure. The small perturbation dynamics about the equilibrium are obtained in the following form:

$$\begin{bmatrix} \ddot{\beta} \\ \ddot{\xi} \\ \dot{\beta} \\ \dot{\xi} \end{bmatrix} = A(\Psi)\begin{bmatrix} \dot{\beta} \\ \dot{\xi} \\ \beta \\ \xi \end{bmatrix} + B(\Psi)u \tag{62}$$

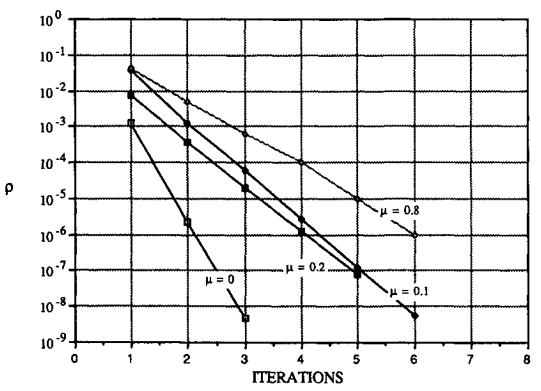

Fig. 1 Effect of advance ratio on outer-loop convergence.

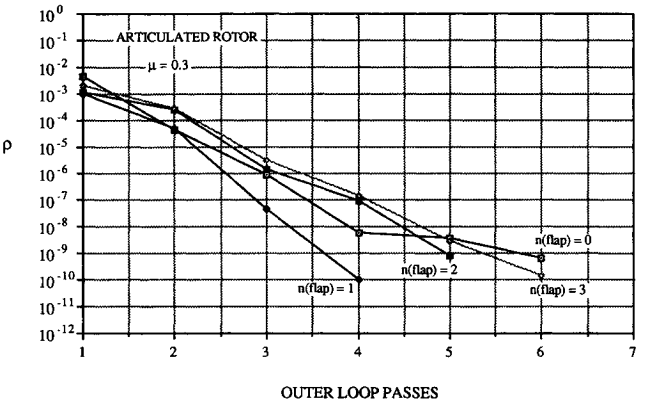

Fig. 2 Effect of flapping Floquet index on outer-loop convergence.

The control input is an actuator at the root of the blade that changes the blade pitch. First, the convergence of the outer-loop calculation is illustrated for cases that range from low to high periodicity level in the coefficients. In addition, the effect that the choice of n_j in Eq. (9) has on outer-loop convergence, and the resulting gain calculation will be shown. Next, the accuracy of the generalized harmonic expansion method is demonstrated. Finally, the results of two case studies will be shown. In the first case, kinematic pitch-lag coupling (θ_ζ in Ref. 14) was set to zero, resulting in a marginally stable open-loop system. In the second case, positive pitch-lag coupling was introduced to destabilize the open-loop lag mode in forward flight.

Convergence Study

Advance ratio is a measure of the level of periodicity. Here, the advance ratio μ is defined as

$$\mu = \frac{V}{\Omega R}\cos(\alpha) \tag{63}$$

where V is the airspeed, Ω the angular rate of the rotor, R the rotor radius, and α the angle of attack of the rotor disk. Increasing μ increases the magnitude of the periodic coefficients in the system dynamics. For this study, the second- and fourth-state variables in Eq. (62) were selected as the output variables, and a performance index in the form of Eq. (16) was chosen. All parameter values were the same as that described for the first case study, with the exception of μ, which is varied. Convergence of the outer-loop calculation is shown in Fig. 1, where a normed measure of the change in the gain matrix is plotted vs the number of outer-loop passes for various values of μ. The norm measure ρ is defined as

$$\rho = |\Delta G|/|G| \tag{64}$$

where the Frobenius matrix norm was used. It is apparent from this figure that, as the level of periodicity increases, the number of outer-loop iterations for a given convergence level increases. However, the algorithm converges reliably for this range of advance ratio. Higher advance ratios were not investigated since $\mu = 0.8$ is well beyond the practical range encountered for current day helicopters.

Figure 2 illustrates the effect that the choice of n_j in Eq. (9) has on the outer-loop convergence. For the in-plane mode ($j = 3,4$), $n_j = 0$ corresponds to the dominant root. For the flapping mode ($j = 1,2$) $n_j = 1$ corresponds to the dominant root. That is, for the flapping root in dimensional form, Ω must be added to the imaginary part of the Poincare exponent calculated from the eigenvalues of the Floquet transition matrix to obtain the root that dominates the response. In Fig. 2, ρ is plotted vs the number of outer-loop passes at $\mu = 0.3$ for $n_j = 0,1,2,3$ in computing the flapping mode. It is observed that the outer loop converges quickest for $n_j = 1$, which corre-

sponds to the root that dominates the flapping response. This minimizes the level of periodicity in $M(\Psi)$, which in turn reduces the need for the outer-loop iteration. However, in each case, the solution converged to the same output feedback gain matrix regardless of the choice of n_j.

Generalized Harmonic Expansion Technique

The generalized harmonic expansion technique (GHET) is used to determine the harmonics of the modal matrix and the harmonics of its inverse, as explained earlier. Here, GHET is compared to a direct numerical integration of Eqs. (9) and (10) using a variable order predictor-corrector integration scheme. An advance ratio of 0.6 is used for comparison, as the dominant periodic effects are more easily observed. The fundamental Poincare exponent was used in Eq. (9). For all comparisons, the relative magnitude of the eigenvector elements were plotted over one rotor revolution. Examples are presented in Figs. 3 and 4.The dashed lines indicate the numerical integration result. The imaginary part of the $d\beta/d\Psi$ element of the flap eigenvector is depicted in Fig. 3. Similar convergence was observed for the corresponding inverse matrix element as shown in Fig. 4. Each element of the approximate modal matrix solution converged using, at most, 10 harmonics at $\mu = 0.6$. For more realistic advance ratios below 0.4, five harmonics produced satisfactory results. As opposed to a least squares procedure, the error is lumped toward the middle of the period and decreases rapidly as more derivatives are matched (more harmonics are used).

Case 1: Zero Pitch-Lag Coupling

For the case studies, the rotor was trimmed at a moderate level flight speed of $V = 80$ kt ($\mu = 0.2$ at $\Omega R = 667$ fps). In the first set of results, the pitch-lag coupling was set to zero. The open-loop flap mode is well damped. However, without a mechanical damper, the in-plane mode damping ratio is only

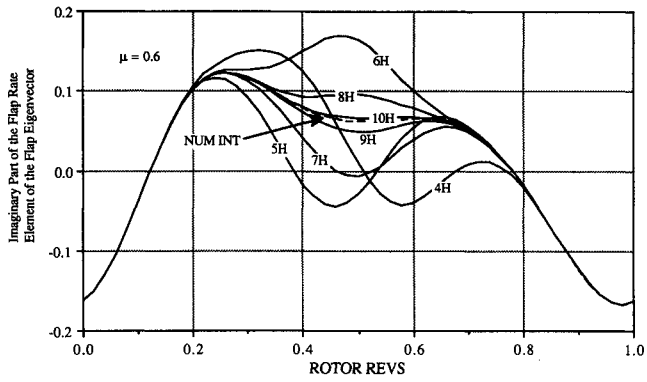

Fig. 3 Harmonic expansion of a Floquet transformation matrix element.

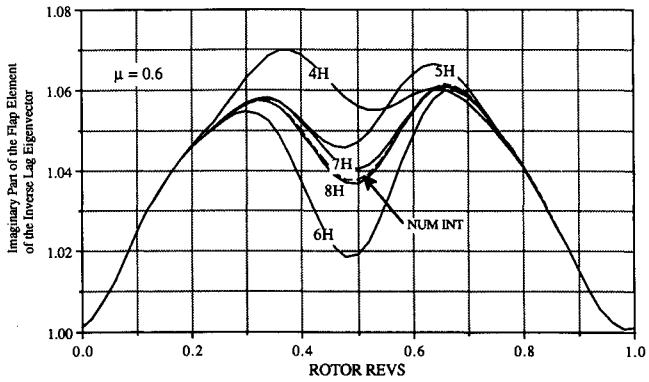

Fig. 4 Harmonic expansion of an inverse Floquet transformation matrix element.

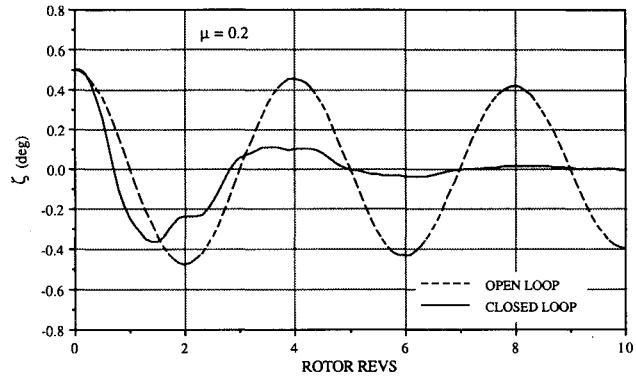

Fig. 5 Lag displacement perturbation response ($\theta_\zeta = 0.0$).

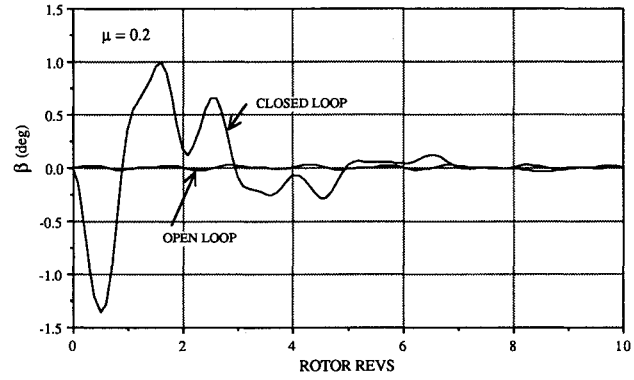

Fig. 6 Flap displacement perturbation response ($\theta_\zeta = 0.0$).

1.4%. Individual blade control was investigated as a means for providing sufficient modal in-plane damping in place of using a mechanical damper.

Consider a controller based only on feedback of lag motion sensor measurements ζ and $d\zeta/d\Psi$. The actual implementation of the control could employ an accelerometer and a root angle transducer mounted on the lag hinge. Lag rate information can be derived using a washed out integration of the acceleration signal, compensated for the centrifugal effect due to hinge offset. A constant coefficient estimator could also be designed using the approach outlined in Ref. 8. The flapping position and rate are assumed to be unavailable for feedback. This reduces the number of sensors required for implementation by a factor of 2. It would be of interest in future work to determine if feedback of lag rate can also be eliminated by extending this approach to the design of constant coefficient dynamic compensators.

After several designs were performed, we settled on the following index of performance:

$$J_e = E_{\eta o}\left\{\int_0^\infty [0.1(\eta_1^2 + \eta_2^2) + 200(\eta_3^2 + \eta_4^2) + 1000\{u^2\}_e]\, d\Psi\right\} \tag{65}$$

Here, η_1 and η_2 are the Floquet states that represent the envelope of flapping mode response and η_3 and η_4 represent the envelope of in-plane mode response. The resulting optimal output feedback individual blade control is

$$u = -g_1\dot{\zeta} - g_2\zeta \tag{66}$$

with

$$g_1 = -1.79, \qquad g_2 = -0.9109 \tag{67}$$

The closed-loop periodic in-plane mode damping ratio is 19.0% relative to 1.4% for the open-loop system. The in-plane

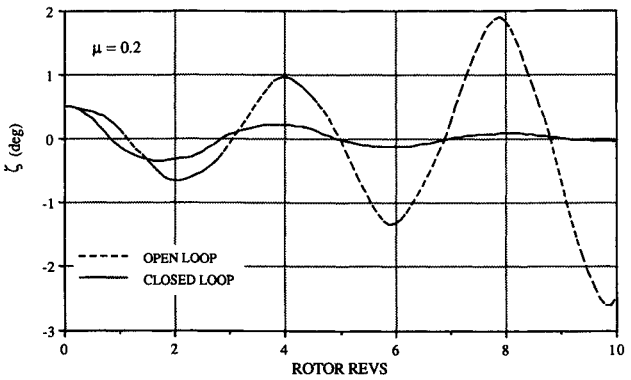

Fig. 7 Lag displacement perturbation response ($\theta_\zeta = 1.0$).

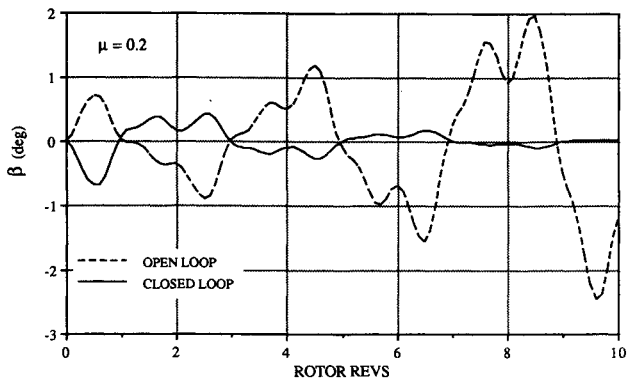

Fig. 8 Flap displacement perturbation response ($\theta_\zeta = 1.0$).

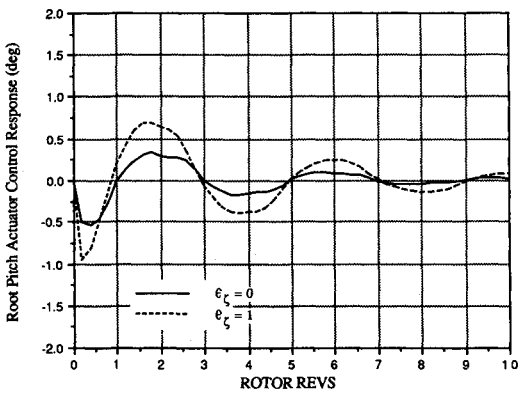

Fig. 9 Root pitch actuator response.

and flapping transient responses to an initial in-plane perturbation are depicted in Figs. 5 and 6, respectively. Both open- and closed-loop system responses are given. It can be seen that use of the modified performance index in Eq. (23) achieves the objective of altering the in-plane response envelope, thus adding modal damping directly to the in-plane mode. The flapping perturbations exhibit higher frequency transients as a consequence of the control input. However, the perturbed flapping response remains small compared to the equilibrium trim values.

Case 2: Positive Pitch-Lag Coupling

Next, the rotor is trimmed with positive pitch-lag coupling. The open-loop lag mode is unstable with $\theta_\zeta = 1.0$. Using the following performance index,

$$J_e = E_{\eta o}\left\{\int_0^\infty [(\eta_1^2 + \eta_2^2) + 750(\eta_3^2 + \eta_4^2) + 1000\{u^2\}_e]\, d\Psi\right\} \quad (68)$$

the resulting output feedback gains are

$$g_1 = 0.611, \qquad g_2 = -1.96 \quad (69)$$

The closed-loop periodic lag mode damping ratio is 16.0%. The in-plane and flapping transient responses due to an initial in-plane perturbation are depicted in Figs. 7 and 8, respectively. Both open-loop and closed-loop system responses are given. Even under the influence of a destabilizing pitch-lag coupling, the control stabilizes the in-plane mode and provides damping characteristics similar to that obtained by using a conventional mechanical damper. From the open-loop response in Fig. 8, it can be seen that even at moderate speeds (moderate advance ratio) a significant level of periodicity is exhibited in the open-loop response. It would be of interest in the future to compare these results with standard output feedback solutions obtained by the MBC transformation,[4] where the system is treated as a equivalent constant coefficient system.

The root pitch actuator response for the two cases is presented in Fig. 9. The maximum amplitude required by the pitch control is 1 deg for a 0.5 deg in-plane perturbation, which appears reasonable relative to the associated closed-loop dynamic characteristics. Additional examples are presented in Refs. 18 and 19, including studies on soft and stiff in-plane hingeless rotors.

Conclusions

The theory of constant gain optimal output feedback has been extended to linear periodic systems. The theory is considerably more complicated than the time-invariant case and requires two levels of iterations in calculating the optimal feedback gains. Constant feedback gains based on plant outputs are calculated by minimizing a linear quadratic performance cost functional that has been modified to allow penalizing the envelope of the state and control responses. For the examples studied to date, the iterations required to calculate these gains appear to converge reliably. The theory has been applied to the control of a helicopter rotor blade in forward flight through individual blade control, and it was determined that lag position and rate information are effective in augmenting lag damping. The effectiveness of the modified performance index in shaping the response envelopes with minimal high-frequency control content is apparent in the numerical results. For this example, the control law implementation is considerably simplified in that the flapping motion is not measured or estimated and the feedback gains are time invariant.

Acknowledgments

This research was supported by the Army Research Office under Grant DAAL3-88-C-0003. Robert Singleton was technical monitor. In addition, thoughtful discussions with David A. Peters at Georgia Institute of Technology are gratefully acknowledged.

References

[1]Moerder, D. D., and Calise, A. J., "Convergence of a Numerical Algorithm for Calculating Optimal Output Feedback Gains," *IEEE Transactions on Automatic Control,* Vol. AC-30, No. 9, 1985, pp. 900-903.

[2]Calise, A. J., and Prasad, J. V. R., "An Approximate Loop Transfer Recovery Method for Designing Fixed Order Compensators," *Journal of Guidance, Control, and Dynamics,* Vol. 35, No. 2, 1990.

[3]Calise, A. J., and Byrns, E. V., Jr., "Robust Fixed Order Dynamic Compensation," AIAA Paper 89-3458, Aug. 1989.

[4]Hohenemser, K. H., and Yin, S. K., "Some Applications of the Method of Multiblade Coordinates," *Journal of the American Helicopter Society,* Vol. 17, No. 3, 1972, pp. 3-12.

[5]Calico, R. A., and Wiesel, W. E., "Control of Time-Periodic Systems," *Journal of Guidance, Control, and Dynamics,* Vol. 7, No. 6, 1984, pp. 671-676.

[6]Calico, R. A., and March, J., "Active Control of Helicopter Blade

Flapping," AIAA Paper 85-1963, Aug. 1985.

[7]Calico, R. A., and Wiesel, W. E., "Stabilization of Helicopter Blade Flapping," *Journal of the American Helicopter Society,* Vol. 31, No. 4, Oct. 1986, pp. 59–64.

[8]McKillip, R. M., "Periodic Control of the Individual Blade Control Helicopter Rotor," *Vertica,* Vol. 9, No. 2, 1985, pp. 199–225.

[9]Hall, W. E., "Application of Floquet Theory to the Analysis of Rotary-Wing VTOL Stability," Guidance and Control Laboratory Rept., Stanford Univ., Stanford, CA, Feb. 1970.

[10]Peters, D. A., and Hohenemser, K. H., "Application of the Floquet Transition Matrix to Problems of Lifting Rotor Stability," *Proceedings of the 26th Annual National Forum of the American Helicopter Society,* June 1970.

[11]Hammond, C. E., "An Application of Floquet Theory to the Prediction of Mechanical Instability," AHS/NASA Ames Specialists' Meeting on Rotorcraft Dynamics, Feb. 1974.

[12]Friedmann, P., and Silverthorn, L. J., "Aeroelastic Stability of Periodic Systems with Application to Rotor Blade Flutter," *AIAA Journal,* Vol. 12, No. 11, 1974, pp. 1559–1565.

[13]Schrage, D. P., and Peters, D. A., "Effect of Structural Coupling Parameters on the Flap-Lag Forced Response of Rotor Blades in Forward Flight Using Floquet Theory," *Vertica,* Vol. 3, No. 2, 1979, pp. 177–185.

[14]Peters, D. A., and Schrage, D. P., "Effect of Structural Parameters on the Flap-Lag Response of a Rotor Blade in Forward Flight," Washington Univ., Interim TR 1, ARO Grant DAAG 29-77-G-0103, St. Louis, MO, July 1978.

[15]Mangus, W., and Winkler, S., *Hill's Equations,* Dover, New York, 1979.

[16]Peters, D. A., and Ormiston, R. A., "Flapping Response Characteristics of Hingeless Rotor Blades by a Generalized Harmonic Balance Method," NASA TN D-7856, Feb. 1975.

[17]Makila, P. M., and Toivonen, H. T., "Computational Methods for Parametric LQ Problems—A Survey," *IEEE Transactions on Automatic Control,* Vol. AC-32, No. 8, 1987, pp. 658–671.

[18]Wasikowski, M. E., Schrage, D. P., and Calise, A. J., "Helicopter Individual Blade Control Through Optimal Feedback," *Proceedings of the AHS National Specialists' Meeting on Rotorcraft Dynamics,* Nov. 1989.

[19]Wasikowski, M. E., "An Investigation of Helicopter Individual Blade Control Using Optimal Output Feedback," Ph.D. Dissertation, Georgia Inst. of Technology, Atlanta, GA, Nov. 1989.